Magnetophoresis of Nonmagnetic, Submicrometer Particles in Magnetic Fluids

Lino Gonzalez, Seif Fateen*, Kenneth Smith and T. Alan Hatton
Department of Chemical Engineering
Massachusetts Institute of Technology, Cambridge, Massachusetts 02139
*Present Address: Nestle R&D Center
Marrysville, Ohio 43040

***Abstract*— We studied the migration of nonmagnetic, submicrometer polystyrene beads submerged in a magnetic fluid in the presence of nonuniform magnetic fields as a potential method for size-based separation of submicrometer, nonmagnetic species. Since the polystyrene beads are much larger than the magnetic fluid nanoparticles, the magnetic fluid was treated as a one-component continuum with respect to the beads. We found that the polystyrene beads will migrate in the direction of decreasing magnetic fields and will focus over a region where the magnetic field or its gradient vanishes, as predicted by our model. The concentration profiles predicted by our model, which has no adjustable or fitted parameters, agree reasonably well with the experimental data both qualitatively and quantitatively.**

I. Introduction

Separations is an active research field in chemical engineering. With increasing advances in technology, the focus has shifted in recent years from macro-scale to micro-scale separations, especially in biological applications. It is very important to be able to separate cells, proteins, DNA, and viruses based on both their physical and chemical/biological properties. Depending on the particle size-range of interest, there are several separation methods that have been used traditionally to separate particles based on size, specific gravity, and chemical properties. Some of the physical methods are summarized in Table 1, where the size 1 μm was chosen arbitrarily to separate small from large particles.

Magnetic fluids have been used in flotation methods to separate particles based on density differences, not size difference, and only on rather large particles ($>$ 1 μm). It was discovered in 1969 that magnetically neutral minerals would experience different magnetic "buoyancy" forces depending on their relative densities [1]. Patented processes were designed where minerals of different densities would reach different equilibrium heights above external magnets, making continuous mineral separation possible [2]. However, these methods are applicable only to materials of different specific gravities and, because of Brownian motion, are not applicable to submicrometer separations.

In recent years there has been extensive work in biological separations using magnetic particles. In most of these processes, small magnetic particles are chemically or physically attached to the nonmagnetic species [3]-[6]. Once the species of interest have been effectively magnetized, magnetic fields are used to move them around the carrier fluid. With this procedure, biological species can be separated because the small magnetic particles would only attach to the species of interest. However, this method is not effective in separating nonmagnetic species that have similar chemical and biological properties. Also, the species would need to be treated at the end of the separation process to remove the magnetic particles.

The present work differs from previous submicrometer separation techniques in that the magnetic particles are not chemically or physically attached to the species of interest. Instead, a magnetic fluid continuum is used to generate a "magnetic pressure" that can be used to move nonmagnetic bodies. Since the particles we are interested in separating are smaller than a micrometer in diameter, buoyancy effects are negligible, so equilibrium separation in space is not possible. Separation is achieved based on a balance between magnetic and drag forces. The nonmagnetic particles reach equilibrium velocities when subjected to external, nonuniform magnetic fields, as opposed to equilibrium heights above a magnet. This work is based on the experimental findings of Fateen [7], who studied the forced diffusion of submicrometer, approximately nonmagnetic polystyrene beads in magnetic fluids. Watarai *et al.* [8] independently studied a similar process, where migration of micrometer-sized polystyrene beads in a paramagnetic $MnCl_2$ solution was described by considering a force balance between viscous drag and forces of magnetic origin. However, water-based magnetic fluids are preferred over paramagnetic salts since they are environmentally and biologically friendly, can achieve much higher magnetic susceptibilities, and can be easily recovered and recycled using High Gradient Magnetic Separation (HGMS). We can also manipulate the magnetization and the ionic strength of the carrier fluid independently in magnetic fluids, which allows for high magnetization without having any of the nonmagnetic particles agglomerate and precipitate out of solution due to charge screening. Our work deals with smaller particles than those studied by [8] present at much larger concentrations. Thus, we model our process as a forced-diffusion process and keep track of concentration profiles, instead of keeping track of individual polystyrene beads. Our model is also able to account for particle-particle interactions, such as electrostatic repulsion between polystyrene beads, which are significant at the concentration levels of interest to us.

TABLE I

SOME WIDELY USED SEPARATIONS PROCESSES FOR DIFFERENT PARTICLE SIZES.

$> 1\ \mu$**m**	$< 1\ \mu$**m**
Filtration	Two phase aqueous partitioning
Cycloning	Ultracentrifugation
Sedimentation	Ultrafiltration
Sieving	Entropic trapping
Centrifugation	Vector chromatography
Flotation	Field flow fractionation

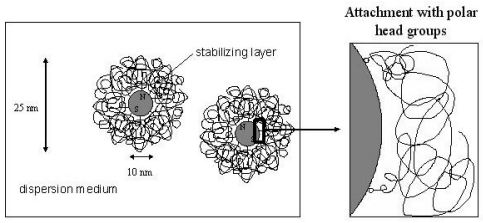

Fig. 1. Magnetic fluid structure

II. MAGNETIC FLUID STRUCTURE

The principal type of ferrofluid used in practice is a colloidal suspension of magnetic, single-domain particles in a liquid carrier, stabilized against agglomeration by a molecular layer of dispersant. Thermal agitation keeps the particles suspended because of Brownian motion, and the coatings prevent the particles from sticking to each other. Most colloidal ferrofluids are synthesized, for they are not commonly found in nature (certain bacteria produce colloidal magnetite, but not in sufficient amounts for commercial use). The two most common methods for preparing a magnetic colloid are size reduction and precipitation [9]. A typical ferrofluid contains 1023 particles per cubic meter and is opaque to visible light.

The most common magnetic material used to make ferrofluids is magnetite (FeO-Fe_2O_3). The average magnetite particle diameter is about 10 nm, with the surfactant or polymer layer making the total diameter about 15-25 nm. Some of the most common carrier fluids include diesters, hydrocarbons, esters, fluorocarbons, and water. The most common carrier for biological applications is water, as it is most compatible with biological materials and the resulting ferrofluid would not be hazardous if trace amounts were left behind in separation processes. In this research, we use a magnetic fluid prepared by precipitation, consisting of a suspension approximately 10 nm magnetite nanoparticles coated with a polymer layer of polyethylene oxide for colloidal stability [10]. A schematic diagram of a coated magnetite particle is shown in Fig. 1. The polymer layer stabilizes our magnetic nanoparticles by a combination of steric hindrance and electrostatic repulsion.

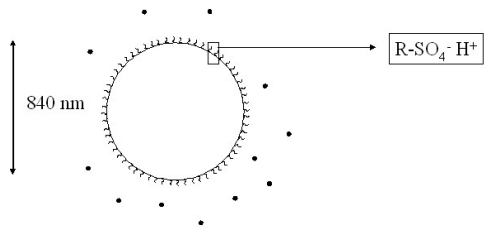

Fig. 2. Polystyrene bead in magnetic fluid "continuum"

III. THEORY

We will start by performing a force balance on a single particle (such as a polystyrene bead) submerged in a ferrofluid in the presence of a spatially nonuniform magnetic field. Since the particles of interest are much bigger than the magnetic fluid nanoparticles, as shown in Fig. 2, the ferrofluid will be treated as a one-component continuum (Fig. 2 is drawn to scale to emphasize the difference in size between the polystyrene beads used in this research and the coated magnetic fluid nanoparticles). This force balance will allow us to study the relationship between the size of the particle and its migration velocity in a ferrofluid continuum. We will then include diffusion effects and some particle-particle interactions to obtain a more complete model describing the forced diffusion of small particles in a magnetic fluid continuum. Since the magnetic nanoparticles that make up the ferrofluid are so small in diameter, the applied magnetic fields will not be strong enough to compete with the Brownian motion of these nanoparticles. The composition of the ferrofluid will therefore remain approximately uniform over time and space. Thus, the density of the ferrofluid continuum will remain approximately constant in time and space.

A. Force Balance on a Single Particle

The force of magnetic origin on a particle p submerged in a ferrofluid f is given by, to leading order,

$$\underline{\mathrm{F}}_m \approx \mu_0 V_p \left(M_p - M_f\right) \underline{\nabla} H \ , \tag{1}$$

where M_f and M_p represent the magnetization of the fluid and the particle, respectively, V_p the volume of the particle, H the magnetic field strength, and μ_0 the permeability of free space [9]. This expression assumes that the ferrofluid behaves as a continuum around the particle p of interest, meaning that the magnetic nanoparticles that make up the ferrofluid must be much smaller than the particle p. The magnetization of the fluid and the particles are assumed to be collinear with the magnetic field, meaning that the above-given force expression is not valid for high-frequency, alternating magnetic fields. Other assumptions include negligible electrical conductivity of the ferrofluid, nearly constant temperature or temperatures much smaller than the Currie temperature of the ferrofluid, constant density, constant composition of the magnetic fluid, small volume fraction of the particles p ($\phi_p \ll 1$), nearly constant H and $\underline{\nabla} H$ over the particle volume V_p, and that the species magnetizations satisfy the conditions

$$\frac{M_p}{H}, \frac{M_f}{H} \ll 1 \ . \tag{2}$$

The purpose of using a ferrofluid is to be able to separate particles that are almost nonmagnetic, since magnetic particles can be easily separated without having to immerse them in a ferrofluid. Thus, we will generally also have that

$$\left|\frac{M_p}{M_f}\right| \ll 1 \ . \tag{3}$$

We will therefore not include the magnetization of the submicrometer particles in our expressions. For cases where the particle magnetization is significant, the magnetization of the fluid appearing in our expressions can simply be replaced by the magnetization difference between the magnetic fluid and the particles of interest.

The magnetization is related to the magnetic field by

$$M = \chi H \ , \tag{4}$$

where χ denotes magnetic susceptibility. In eq. (1), we have allowed for the particle and the ferrofluid to be nonlinear, meaning that $\chi = \chi(H)$. This is very important since magnetic fluids are not magnetically linear, as seen in Fig. 3. Although more rigorous equations are available to relate χ to H, we decided to use the simple, empirical relationship

$$\chi = \frac{M_s}{H_T + H} \ , \tag{5}$$

where M_s is the saturation magnetization of the fluid (the magnetization at infinite applied magnetic field) and H_T is the magnetic field strength at which $M = M_s/2$. As shown in Fig. 3, this empirical relationship fits the experimental data very well and its simplicity allows for fast numerical solutions to our model equations. In Fig. 3, a negative value of the magnetic field is used to indicate that the field was applied in the opposite direction. The resulting magnetization is symmetric, as expected. When using eq. (5), the value of H is the magnitude of the applied field. The values used to generate the curve are $M_s = 665$ A/m and $H_T = 6.2 \times 10_4$ A/m. Finally, eq. (1) is valid whether the particle p is stationary or migrating at a velocity $\underline{\mathrm{u}}_p(t)$, as long as the assumptions described above are satisfied and the particle is small enough so that inertial effects are negligible.

Equation (1) tells us that the force of magnetic origin acting on particles submerged in a ferrofluid is proportional to their volume, the difference in magnetization between the particles and the ferrofluid continuum, and to the magnetic field gradient. This means that nonmagnetic particles will be "pushed" in the direction of decreasing magnetic fields until either the magnetic field or its gradient vanishes (the force of magnetic origin will vanish when the magnetic field is zero, since the fluid magnetization will also be zero at that point). All sufficiently large nonmagnetic particles will migrate in the direction in which the magnetic field is decreasing and eventually focus in a region where the magnetic field or its gradient vanishes (since gravitational effects are negligible), regardless of their relative sizes. Thus, size separation is not possible when the particles reach their equilibrium position.

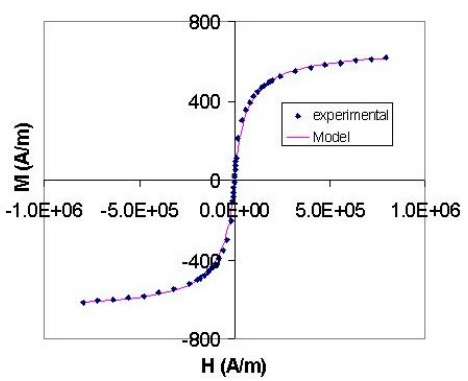

Fig. 3. Magnetization of 1% magnetic fluid versus applied magnetic field

However, since this force of magnetic origin is also proportional to the particle volume, different-sized particles will migrate toward the equilibrium positions at different velocities, meaning that dynamic separation in space is possible even if static separation is not.

B. Forced Diffusion

Since the particles of interest are about a micrometer in diameter, Brownian motion and particle-particle interactions are significant and must be accounted for. To achieve this, we will introduce a diffusion "force," given as the negative of the gradient of the chemical potential of the particle at constant temperature. A balance between this diffusive "force," the viscous drag force on a particle, the gravitational force, and the force of magnetic origin gives (to leading order)

$$\begin{gathered} -\tfrac{1}{N_a}\left(\underline{\nabla}\zeta_p\right)_T + 6\pi\eta a\left(\underline{\mathrm{v}}^*\text{-}\underline{\mathrm{u}}_p\right) + \rho_p V_p \underline{\mathrm{g}} \\ -\mu_0 V_p M_f \underline{\nabla} H = \underline{0} \ , \end{gathered} \tag{6}$$

where N_a is Avogadro's number, ζ_p is the chemical potential of the particle, T is temperature, η is the viscosity of the fluid, a is the hydrodynamic radius of the particle, $\underline{\mathrm{u}}_p$ is the velocity of the particle relative to a fixed reference frame, $\underline{\mathrm{v}}^*$ is the volume-average velocity of the particle, ρ_p is the density of the particle, and $\underline{\mathrm{g}}$ is the gravitational constant vector. Here the chemical potential is not a function of H since we have introduced the force of magnetic origin as an external force on the $particle$, not as a force density on the system. The above expression can be rearranged to give

$$\underline{\mathrm{u}}_p - \underline{\mathrm{v}}^* = \frac{\left\{ \begin{array}{c} -\tfrac{1}{N_a}\left(\underline{\nabla}\zeta_p\right)_T + \rho_p V_p \underline{\mathrm{g}} \\ \\ -\mu_0 V_p M_f \underline{\nabla} H \end{array} \right\}}{6\pi\eta a} \ . \tag{7}$$

Using the Stokes-Einstein equation for the diffusion coefficient results in

$$\underline{\mathrm{u}}_p - \underline{\mathrm{v}}^* = -\frac{D_p}{RT}\left\{ \begin{array}{c} \left(\underline{\nabla}\zeta_p\right)_T - \rho_p \overline{V}_p \underline{\mathrm{g}} \\ \\ +\mu_0 \overline{V}_p M_f \underline{\nabla} H \end{array} \right\} \ , \tag{8}$$

where D_p denotes the diffusion coefficient of particle p in the ferrofluid f, R is the gas constant, and $\overline{V}_p$ is the molar volume of the particle. We can now obtain the diffusive flux relative to the molar-average velocity, given by

$$\underline{\mathrm{J}}_p^* \equiv C_p\left(\underline{\mathrm{u}}_p - \underline{\mathrm{v}}^*\right) \tag{9}$$

$$= -\frac{C_p D_p}{RT}\left\{\begin{array}{c}(\underline{\nabla}\zeta_p)_T - \rho_p \overline{V}_p \underline{\mathrm{g}} \\ \\ +\mu_0 \overline{V}_p M_f \underline{\nabla} H\end{array}\right\}, \tag{10}$$

where C_p is the molar concentration of the particles. This can be rearranged to give

$$\underline{\mathrm{J}}_p^* = -\frac{D_p}{RT}\left\{\begin{array}{c}C_p(\underline{\nabla}\zeta_p)_T - \phi_p \rho_p \underline{\mathrm{g}} \\ \\ +\phi_p \mu_0 M_f \underline{\nabla} H\end{array}\right\}, \tag{11}$$

where ϕ_p is the volume fraction of particles in the mixture.

To interpret the result obtained, let's examine (11) in the case were the chemical potential and gravity effects are negligible. For a small, fixed number of spherical particles n, we have that the volume fraction is proportional to a^3, the diffusion coefficient is proportional to the radius a, so the flux of particles relative to the fluid is proportional to a^2, as expected from a balance between the force of magnetic origin (proportional to a^3) and the drag force (proportional to a). It is this flux dependence on particle size that makes dynamic, size-based separation of particles in space possible.

In (11), a large portion of the physics involved in this forced-diffusion process are contained in the chemical potential ζ_p, which can be written as

$$\zeta_p = \zeta_0(T,P) + RT\ln x_p + \zeta_p^{ex}(T,P,x_p)\ . \tag{12}$$

Here ζ_0 is the chemical potential is a reference chemical potential at the temperature T and pressure P of interest, x_p is the mole fraction of particles p, and ζ_p^{ex} is the excess chemical potential. We can therefore write

$$(\underline{\nabla}\zeta_p)_T = \overline{V}_p \underline{\nabla} P + \frac{RT}{x_p}\underline{\nabla} x_p + \underline{\nabla}\zeta_p^{ex}(T,P,x_p)\ . \tag{13}$$

For the process of interest to us, pressure drops due to fluid flow are negligible in comparison to hydrostatic pressure gradients, so we will therefore have

$$\underline{\nabla} P \approx \rho \underline{\mathrm{g}}\ . \tag{14}$$

Inserting these result back into (10) gives

$$\underline{\mathrm{J}}_p^* = -\frac{D_p}{RT}\left\{\begin{array}{c}CRT\underline{\nabla} x_p + C_p \underline{\nabla}\zeta_p^{ex}(T,P,x_p) \\ \\ +(\phi_p - w_p)\rho \underline{\mathrm{g}} \\ \\ +\phi_p \mu_0 M_f \underline{\nabla} H\end{array}\right\}, \tag{15}$$

where C is the total concentration of the fluid. For our system of interest, the density of the polystyrene beads and the dilute magnetic fluid carrier are equal, so that the gravitational buoyancy term appearing in (15) $(\phi_p - w_p)\rho\underline{\mathrm{g}}$ is completely negligible. Even when substantial density differences are present, the gravitational buoyancy term in this expression is usually much smaller than the molecular diffusion term $\underline{\nabla} x_p$ for small particles. We thus have that, for our case of interest,

$$\underline{\mathrm{J}}_p^* = -\frac{D_p}{RT}\left\{\begin{array}{c}CRT\underline{\nabla} x_p + C_p \underline{\nabla}\zeta_p^{ex}(T,P,x_p) \\ \\ +\phi_p \mu_0 M_f \underline{\nabla} H\end{array}\right\}. \tag{16}$$

For an ideal system in the absence of magnetic fields, we see that

$$\underline{\mathrm{J}}_p^* = -CD_p \underline{\nabla} x_p\ , \tag{17}$$

which is Fick's law for the molar flux relative to the molar-average velocity [11]. The other terms in (16) account for flux due to nonidealities (such as particle-particle interactions) and magnetic effects. Finally, for a binary system, the molar flux relative to the mass-average velocity is given by

$$\underline{\mathrm{J}}_p = \frac{W_f C}{\rho}\underline{\mathrm{J}}_p^* \tag{18}$$

$$= -\frac{W_f C D_p}{\rho RT}\left\{\begin{array}{c}CRT\underline{\nabla} x_p + C_p \underline{\nabla}\mu_p^{ex} \\ \\ +\phi_p \mu_0 M_f \underline{\nabla} H\end{array}\right\}, \tag{19}$$

where W_f is the molecular weight of the magnetic fluid solvent.

Now that we have an expression for the molar flux, we can obtain the governing equation for the evolution of the concentration profile of the particles. At constant density and in the absence of convection (no mass-average velocity), the concentration profile is governed by

$$\frac{\partial C_p}{\partial t} + \underline{\nabla}\cdot\underline{\mathrm{J}}_p = 0\ , \tag{20}$$

where the molar concentration and the mole fraction are related by $C_p = x_p C$ and J_p is given by eq. (19).

C. Nonidealities

In our derivation, we have allowed for an excess chemical potential to describe effects that cannot be captured by ordinary diffusion. We have found experimentally that ordinary diffusion is too small to compete with the magnetic effects, so there must be other mechanisms that are affecting the evolution of the concentration profiles for the polystyrene beads. The ideal chemical potential assumes that the individual particles occupy zero volume and that there in no interaction between particles. Since we know that the polystyrene beads have a finite volume and that there is electrostatic repulsion between the beads, we assumed that the excess chemical potential should consist of mostly excluded-volume effects and electrostatic-repulsion effects. Furthermore, since volume-exclusion effects are so much smaller than electrostatic effects at the conditions of interest to us, we neglected volume exclusion and only focused on electrostatic effects. The total excess chemical potential of species p in solvent s was calculated to be

$$\zeta_p^{ex} \approx 16\pi^2 \varepsilon \Psi_0^2 a^2 \kappa^{-2}\left[1 + 2\kappa a\right] N_a^2 C x_p\ , \tag{21}$$

where we have used the fact that $\phi_p \ll 1$ and that the volume exclusion contribution is considerably smaller than the electrostatic contribution [7]. In this expression, ε is the electric permittivity of the fluid, Ψ_0 is the electric potential at the surface of the particles, κ^{-1} is the Debye length, and N_a is Avogadro's number.Thus, we have that, at constant density,

$$\underline{\nabla}\zeta_p^{ex} = \frac{16\pi^2\varepsilon\Psi_0^2 a^2\kappa^{-2}\left[1+2\kappa a\right]N_a^2C^2W_s}{\rho}\underline{\nabla}x_p \ . \quad (22)$$

In deriving these expressions, we have assumed that the double-layer theory, which is strictly and electro-quasi-static concept, is still valid for our system. Since magnetic fluids are non-conducting, our magnetic fields do not vary in time, and the migration of the polystyrene beads is slow enough not induce any significant fields, the equations used and assumptions made in the double-layer theory are indeed valid. By introducing a constant defined as

$$\widetilde{\Psi}_0^2 = \frac{16\pi^2\varepsilon\Psi_0^2 a^2\kappa^{-2}\left[1+2\kappa a\right]N_a^2CW_s}{\rho RT} \ , \quad (23)$$

we can rewrite the molar diffusive flux relative to the mass-average velocity as

$$\underline{\mathrm{J}}_p = -\frac{W_f C D_p}{\rho RT}\left\{\begin{array}{c} CRT\underline{\nabla}x_p\left(1+Cx_p\widetilde{\Psi}_0^2\right) \\ \\ +\phi_p\mu_0 M_f\underline{\nabla}H \end{array}\right\} . \quad (24)$$

IV. Experimental Setup

The experimental arrangement used in this research is shown schematically in Fig. 4. Fluorescently-tagged latex beads were used as the nonmagnetic particles. These beads emit fluorescent light when excited by light at the correct frequency. The excitation source was a 200-W mercury lamp, and the desired excitation frequency was selected using appropriate filters. A digital camera was used to capture images of the emitted light, whose intensity is proportional to the concentration of beads. Thus, we were able to monitor concentration profiles by measuring the intensity of the emitted light. The concentration of the magnetic fluid used in our experiments was a dilute 1% by mass of magnetite, since a more concentrated magnetic fluid would be too opaque and block out polystyrene fluorescence.

Fig. 5 shows a schematic representation of the experiments performed. A capillary tube with an inner diameter of 350 μm and an outer diameter of 500 μm was filled with a mixture of 1% by mass magnetite (stabilized by a polymer layer) and 0.4% by mass of fluorescently-tagged polystyrene beads. The remaining 98.6% of the mass consisted of deionized water and the polymer layer surrounding the magnetite particles. At time $t = 0$, two 12.7 mm diameter magnets where placed at a position $z = 0$, with a 7 mm gap between the magnets. Two different sizes of polystyrene beads where used: 510 nm and 840 nm in diameter. The setup described in Fig. 4 was used to monitor the concentration profile of the polystyrene beads as a function of time. All of the experiments were performed at room temperature.

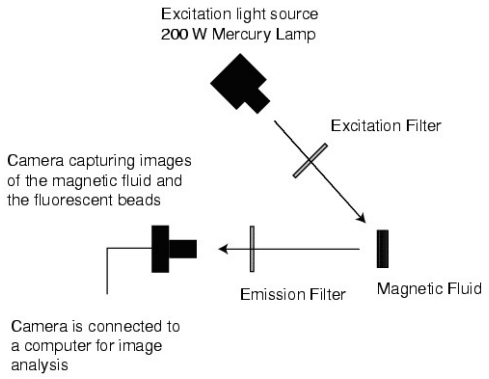

Fig. 4. Experimental setup

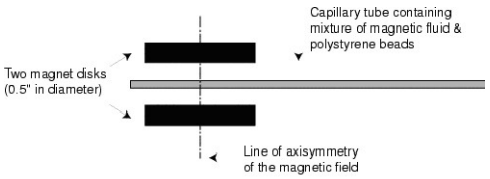

Fig. 5. Magnetophoresis experiment

V. Results

Experiments were performed using different bead sizes. Here we show and analyze the results obtained for 840 nm beads as well as 510 nm beads with the experimental setup described in Fig. 5. The magnetic field profile generated by the two magnets is given in Fig. 6, where z is the distance along the center of the capillary tube and $z = 0$ is the center of the two magnets (the plane of symmetry).

A. Experimental Results

The experimental data for the 840 nm and the 510 nm beads have been plotted in Fig. (7) and (8), respectively. The plots are normalized by the initial concentration of the polystyrene beads. The results are plotted at four different times: 100 s, 490 s, 1080 s, and 4630 s. As expected, the latex beads migrated away from the region of high magnetic fields and settled in the region where the magnetic field and its gradient vanished. Also as expected, the 840 nm beads migrated faster and reached a

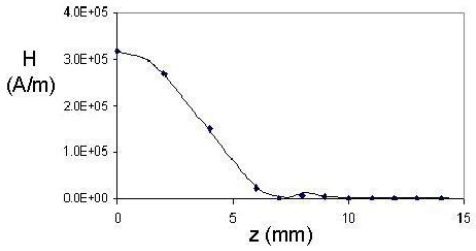

Fig. 6. Magnetic field profile

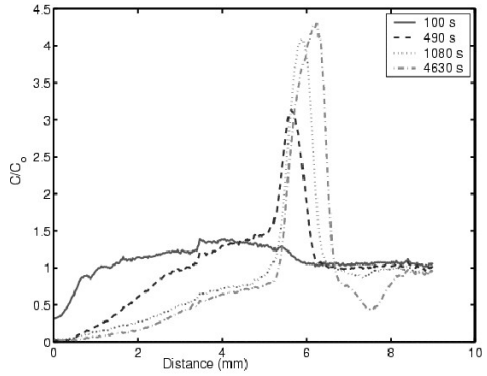

Fig. 7. Experimental concentration profile for 840 nm particles

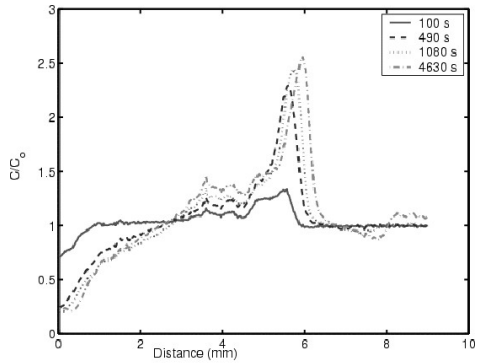

Fig. 8. Experimental concentration profile for 510 nm particles

higher peak concentration, since the magnetic effects become more significant than the diffusive and electrostatic effects with increasing particle size. If the experiments were performed over a larger period of time, the peak that reaches a maximum at about 4000 seconds would eventually decay toward the positive z direction, since there is no magnetic force in this region and the only active terms in the molar flux are diffusion and electrostatic repulsion. However, due to the rather large size of the particles, this process would take days to complete.

B. Comparison with Model

Equation (20) was solved in one spatial dimension and time to predict the concentration profiles for the experimental conditions described above. The computer program MATLAB was used to perform the numerical integration. The initial condition used was a constant concentration profile for all z. The boundary conditions used were no flux at $z = 0$ and $x_p = x_p(t = 0)$ at $z = 15$ mm. The latter condition was used since the experimental results suggest that the particle concentration will not vary significantly at this point. A list of the parameters used is given in Table 2. Since the volume fraction of latex beads never exceeds 0.02 (5 times the original concentration) and since the magnetic fluid only contains 0.01 weight fraction of magnetite, we assumed that the concentration and viscosity of the mixture can be approximated by the concentration and viscosity of pure water, respectively. The densities of the magnetic fluid and the latex beads are both 1050 Kg/m^3, so the density of the mixture is also 1050 Kg/m^3. The molecular weight of the polystyrene beads was calculated from the weight of 6.022 $\times 10^{23}$ beads of the given diameter, and the diffusion coefficients were calculated using the Stokes-Einstein equation,

$$D_p = \frac{RT}{6\pi\eta a N_a} \ . \tag{25}$$

The results of the numerical integrations are plotted at the times of interest for the 840 nm and the 510 nm particles in Fig. (9) and (10), respectively.

TABLE II
PARAMETERS USED IN MODEL

PARAMETER	VALUE
R	8.314 J/(mol·K)
T	298 K
μ_0	$4\pi \times 10^{-7}$ H/m
ε	6.95×10^{-10} F/m
Ψ_0	0.031 V
κ^{-1}	9.6×10^{-7} m
M_s	665 A/m
H_T	6.2×10^4 A/m
ρ	1050 Kg/m^3
η	1.0×10^{-3} Kg/(m·s)
C	5.8×10^4 mol/m^3
W_s	1.8×10^{-3} Kg/mol
W_{840}	1.96×10^8 Kg/mol
W_{510}	4.39×10^7 Kg/mol
D_{840}	5.20×10^{-13} m^2/s
D_{510}	8.56×10^{-13} m^2/s
x_{840}	3.67×10^{-13}
x_{510}	1.64×10^{-12}

C. Discussion

As we can see from comparing the results obtained from our diffusion model to the experimental data, the model predicts the correct trends and the correct height of the concentration peak. This is very encouraging since the model does not contain any adjustable or fitted parameters. The expressions used for the magnetic force and the electrostatic repulsion are only leading-order approximations. Several of the discrepancies observed between the experiments and the model can be explained by examining the approximations made in deriving the model. First, we assumed that the concentration of the magnetic fluid would not vary at all during the experiment. This approximation is not strictly valid in the neighborhood of $z = 0$ due to the high magnetic forces present there. We also neglected any interactions between the magnetic nanoparticles and the latex beads. Since the magnetic nanoparticles are stabilized with a polymer that will have a net negative charge (the latex beads also have a negative charge when suspended in water), these interactions may become significant. Finally, the

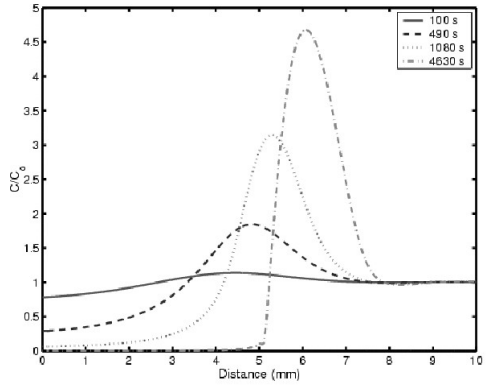

Fig. 9. Predicted concentration profile for 840 nm particles

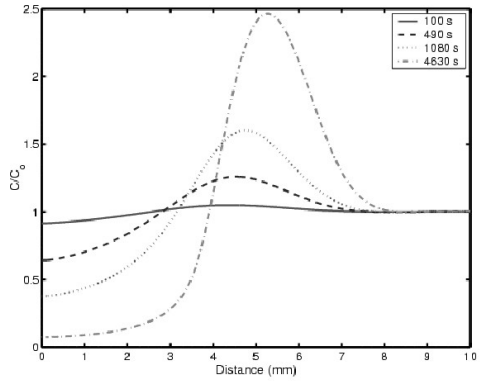

Fig. 10. Predicted concentration profile for 510 nm particles

magnetic fluid nanoparticles are not completely monodisperse, so in practice the larger magnetic nanoparticles will tend to concentrate in the vicinity of $z = 0$. The combination of these effects may explain the discrepancies observed in the neighborhood of $z = 0$.

We can clearly see form our results that our model over-predicts the thickness of the concentration peak. Our model only accounts for diffusion and electrostatic effects, and only to leading order. We will need to account for other types of interactions to obtain a better fit between the experimental and the predicted results. The experimental data also shows a "dip" in the concentration profile to the right of the concentration peak. This is not predicted by the model and we do not know if this is a real effect or an error in experimental measurements. In our experimental setup, the light from the mercury lamp shines on the sample at an angle, and it is possible that the high concentration of beads at the peak will block the light and prevent it from reaching the fluorescently-tagged latex beads just to the right of the peak. We are developing a new setup that uses a dichroic mirror to deflect the light coming from the mercury lamp so that it shines on our sample at a right angle.

In summary, our model is able to predict the correct trends in the concentration profile of polystyrene beads and the correct numerical value for the concentration peaks. To obtain a better fit with the experimental data, some of our simplifications need to be relaxed, and the experimental setup needs to be modified in order to obtain more accurate experimental data.

ACKNOWLEDGMENT

The authors would like to thank the Singapore-MIT Alliance (SMA) for partial financial support of this research.

REFERENCES

[1] R. E. Rosensweig, "Material separation using ferromagnetic liquid techniques," U.S. patent 3 700 595, 1969.
[2] J. Shimoiizaka, K. Nakatsuka, T. Fujita, and A. Kounosu, "Sink-float separators using permanent magnets and water based magnetic fluid," *IEEE Trans. Magnetics*, vol. MAG-16 (2), pp. 368-371, 1980.
[3] M. Berger, J. Castelino, R. Huang, M. Shah, and R. H. Austin, "Design of a microfabricated magnetic separator," *Electrophoresis*, vol. 22, pp. 3883-3892, Oct. 2001.
[4] J. Choi, T. M. Liakopoulos, and C. H. Ahn, "An on-chip magnetic bead separator using spiral electromagnets with semi-encapsulated permalloy," *Biosensors and Bioelectronics*, vol. 16, pp. 409-416, Aug. 2001.
[5] P. A. Liberti and B. P. Feeley, "Microtitre well cell-separation with bioreceptor ferrofluids in high-gradient magnetic separations," *FASEB Journal*, vol. 5 (6), a1690 part 3, 1990.
[6] S. Roath, R. Smith, and J. H. P. Watson, "High-gradient magnetic separation in blood and bone-marrow processing," *J. Magn. Magn. Mater.*, vol. 85 (1-3), pp. 285-289, Apr. 1990.
[7] S. Fateen, "Magnetophoretic focusing of submicron particles dispersed in a polymer-based magnetic fluid," Ph.D. dissertation, Dept. Chem. Eng., Massachusetts Institute of Technology, Cambridge, MA 2002.
[8] H. Watari and N. Makoto, "Magnetophoretic Behavior of Single Polystyrene Particles in Aqueous Manganese(II) Chloride," *Anal. Sci.*, vol. 17, pp. 1233-1236, Oct. 2001.
[9] R. E. Rosensweig, *Ferrohydrodynamics*. New York, NY: Cambridge University Press, 1985, pp. 153-157.
[10] G. Moeser, K. A. Roach, W. H. Green, P. E. Laibinis, and T.A. Hatton, *Ind. Eng. Chem. Res.*, vol. 41 (19), pp. 4739-4749, Sep. 2002.
[11] W. M. Deen, *Analysis of Transport Phenomena*. New York, NY: Oxford University Press, 1998, pp. 4-5.